



Contents lists available at ScienceDirect

## Journal of Volcanology and Geothermal Research

journal homepage: [www.elsevier.com/locate/jvolgeores](http://www.elsevier.com/locate/jvolgeores)

## El Chichon: The genesis of volcanic sulfur dioxide monitoring from space

Arlin Krueger<sup>a,\*</sup>, Nickolay Krotkov<sup>b</sup>, Simon Carn<sup>a</sup><sup>a</sup> Joint Center for Earth Systems Technology, University of Maryland, Baltimore County, 1000 Hilltop Circle, Baltimore, MD 21250, United States<sup>b</sup> Goddard Earth Sciences & Technology Center, University of Maryland, Baltimore County, 1000 Hilltop Circle, Baltimore, MD 21250, United States

## ARTICLE INFO

## Article history:

Accepted 12 February 2008

Available online xxx

## Keywords:

volcanism  
explosive eruptions  
sulfur dioxide  
remote sensing  
El Chichon  
TOMS

## ABSTRACT

The 1982 eruption of El Chichon inspired a new technique for monitoring volcanic clouds. Data from the Total Ozone Mapping Spectrometer (TOMS) instrument on the Nimbus-7 satellite were used to measure sulfur dioxide in addition to ozone. For the first time precise data on the sulfur dioxide mass in even the largest explosive eruption plumes could be determined. The plumes could be tracked globally as they are carried by winds. Magmatic eruptions could be discriminated from phreatic eruptions. The data from El Chichon are reanalyzed in this paper using the latest version of the TOMS instrument calibration (V8). They show the shearing of the eruption cloud into a globe-circling band while still anchored over Mexico in three weeks. The measured sulfur dioxide mass in the initial March 28 eruption was 1.6 Tg; the April 3 eruption produced 0.3 Tg more, and the April 4 eruptions added 5.6 Tg, for a cumulative total of 7.5 Tg, in substantial agreement with estimates from prior data versions. TOMS Aerosol Index (absorbing aerosol) data show rapid fallout of dense ash east and south of the volcano in agreement with Advanced Very High Resolution Radiometer (AVHRR) ash cloud positions.

© 2008 Elsevier B.V. All rights reserved.

## 1. Introduction

In 1982, anomalously high total ozone appeared above Mexico in data from the Total Ozone Mapping Spectrometer (TOMS) on the Nimbus-7 satellite at the same time as the eruption of El Chichon (Krueger, 1983). After 6 centuries of repose, El Chichon erupted violently on March 28 through April 4, 1982. This volcano and the eruptions are well documented in terms of chronology, petrology, stratigraphy, and motion of the ash clouds (Robock and Matson, 1983; Matson, 1984; Varekamp et al., 1984; Luhr et al., 1984; Rose et al., 1984; Sigurdsson et al., 1984). The detailed behavior of the April 4 eruption gas and ash clouds was analyzed by Schneider et al. (1999) using data from TOMS and AVHRR instruments. The atmospheric effects of the eruption were reviewed by Hofmann (1987).

The TOMS instrument (Heath et al., 1975; Krueger, 1989), launched in October 1978, was designed, as its name implies, to determine the spatial structure in total ozone through daily, contiguous mapping of the earth. Prior ozone data from ground stations showed high variability with time scales similar to meteorological changes, but the relations with weather were elusive because of the sparse distribution of stations. The TOMS was built with the best spatial resolution available with 1970's technology (50 km at nadir) to resolve anticipated gradients in total ozone. The spacecraft data rate also limited the spectral coverage to 6 discrete ultraviolet wavelengths for total ozone soundings (Dave and

Mateer, 1967). The contiguous mapping proved to be at least as valuable for volcanology as for atmospheric ozone.

The TOMS total ozone algorithm was developed with the assumption that ozone was the only absorbing gas at near UV wavelengths (310–380 nm). Other gases were ignored because they were normally present in far lower optical depths than ozone. In 1982, the strange cloud of apparent high total ozone over Mexico (Fig. 1a) at the time of the El Chichon (small black triangle on Fig. 1a) eruption required an explanation. Krueger (1983) showed that the spectral anomalies were consistent with sulfur dioxide, making it the most likely volcanic constituent to account for the anomalous absorption. A simple scheme to separate sulfur dioxide from ozone absorption was proposed. The sulfur dioxide absorption spectrum overlaps the ozone spectrum but with different structure. Other gases, such as carbon disulfide, also absorb at these wavelengths, but would produce different spectral anomalies. Sulfur dioxide amounts were estimated from the deviation of the observed radiances from an interpolation of unperturbed radiances on either side of the volcanic cloud. Agreement at the two TOMS wavelengths within the SO<sub>2</sub> band was within 10%, but absolute amounts were not certain because at the time only room temperature SO<sub>2</sub> cross sections had been measured (Wu and Judge, 1981) while the cloud temperatures were near -50 °C. An average column SO<sub>2</sub> amount over the cloud, multiplied by the cloud area obtained from the TOMS images yielded a total mass in the April 5th cloud of 3.3 Tg. New cross section data at low temperatures (McGee and Burris, 1987) are now used to produce more accurate results.

With the contiguous coverage and moderate spatial resolution of TOMS it now became possible to measure the mass of sulfur dioxide in

\* Corresponding author. Tel.: +1 410 455 8906; fax: +1 410 455 5868.  
E-mail address: [akrueger@umbc.edu](mailto:akrueger@umbc.edu) (A. Krueger).

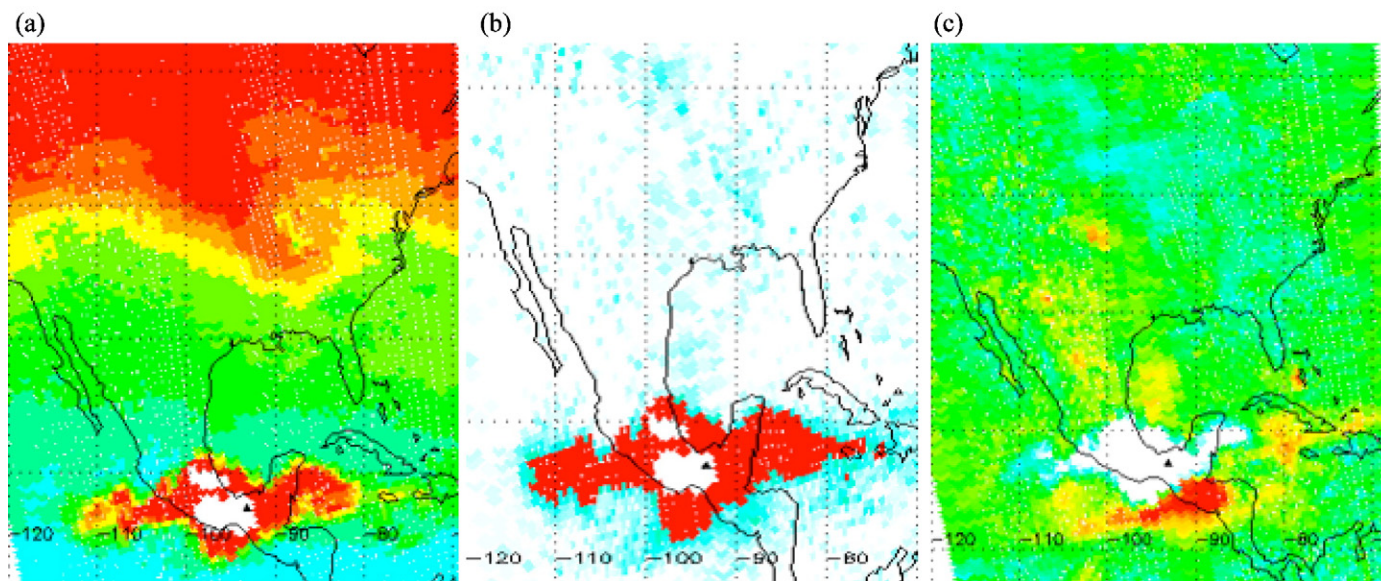


Fig. 1. a. Image of the total ozone field from the Nimbus-7 satellite Total Ozone Mapping Spectrometer (TOMS) on April 5, 1982 showing anomalous high ozone retrievals (yellow, red, white colors) above Mexico. Normal tropical ozone levels are the blue and green colors while the red and yellow colors across the northern United States are usual midlatitude ozone values. The volcanic anomaly is due to failure of the ozone retrieval algorithm to account for sulfur dioxide absorption. El Chichon's location is shown by the black triangle over southern Mexico. All Nimbus-7 data are taken about an hour before local noon. b. A revised TOMS ozone data production algorithm flags  $\text{SO}_2$  contaminated ozone retrievals with a sulfur dioxide index (SOI). The red area represents SOI levels above 100 DU (1 mm of pure  $\text{SO}_2$  gas at STP conditions) in the April 5, 1982 El Chichon eruption cloud. This algorithm fails for greater than 205 DU of  $\text{SO}_2$  (white areas in the center of the cloud). c. A TOMS Aerosol Index (AI) is a measure of absorbing aerosol optical depths. This image of the April 5, 1982 eruption shows ash clouds in yellow and red colors. The white central cloud region represents failed AI retrievals from large sulfur dioxide amounts. (For interpretation of the references to color in this figure legend, the reader is referred to the web version of this article.)

eruption clouds that were far too large to be assessed from the ground or from aircraft. This began an extended effort to improve the sulfur dioxide retrieval algorithm and to map all of the volcanic eruption clouds in the TOMS database.

The volcanic sulfur dioxide data are derived in part from the standard Level 2 TOMS datasets and in part from special off-line analysis of the Level 1 orbital data. The special analysis is required whenever high sulfur dioxide amounts are present. The retrieval algorithm is implemented in the TOMSPLOT utility software.

## 2. Volcanic products in TOMS production data

Three useful products are available for eruption analysis in the standard TOMS output data, available in Level 2 (orbital) format from the Goddard Distributed Active Archive Center (DAAC) (McPeters et al., 1993). They include total ozone anomalies, Sulfur Dioxide Index, and Aerosol Index. Over the years the standard TOMS data production has gone through eight versions as the ozone algorithm and instrument calibration were updated. However, the production algorithm only calculates effective total ozone, as illustrated in Fig. 1a using the most recent (Version 8) ozone data (Bhartia and Wellemeyer, 2004). The ozone anomaly due to sulfur dioxide on April 5, 1982 is the irregular red/white area over Mexico. Sulfur dioxide clouds always produce erroneously high total ozone. Thus, even small eruptions may appear as anomalous bumps in the ozone field, especially in the tropics, where the ozone is nearly constant.

A second useful product is the Sulfur Dioxide Index (SOI), designed for flagging contaminated ozone retrievals (Fig. 1b). The SOI has been calibrated to yield approximately correct sulfur dioxide amounts for small  $\text{SO}_2$  amounts. SOI is the radiance residual at a short TOMS wavelength from the best total ozone solution obtained at a longer wavelength. However, if the ozone is wrong, the residual is wrong. So, SOI is valid only for low  $\text{SO}_2$  amounts (<30 Dobson units). Nevertheless, SOI is a convenient tool for locating volcanic clouds [Note: 1 Dobson unit =  $2.69 \times 10^{16}$  molecules/cm<sup>2</sup>].

A third standard V8 TOMS parameter, Aerosol Index (AI), a residual at a long TOMS wavelength, is a measure of the deviation of the backscattered spectrum from a Rayleigh spectrum. The light scattering properties of the

atmosphere at UV wavelengths are dominated by Rayleigh scattering, except when absorbing aerosols, such as volcanic ash, are present. Ash produces large positive AI deviations, shown in red in Fig. 1c just south of the large white area over the El Chichon sulfur dioxide cloud. Near zero AI values are in green and blue colors. The white areas are invalid retrievals due to the effect of large  $\text{SO}_2$  amounts on the ozone retrievals.

The TOMS Aerosol Index has proved very useful for tracking volcanic ash clouds, which are a hazard to aviation. Other absorbing aerosols, such as dust and smoke, can produce the same signal as ash, so that AI is not unique to volcanic clouds. However, sulfur dioxide is unique to volcanic clouds, so that a combination of the two parameters is a valuable tool for aviation safety.

## 3. Off-line sulfur dioxide retrieval algorithms

In the original analysis of the El Chichon eruption it became obvious that the TOMS total ozone algorithm could not be used when volcanic clouds were present. In fact, because sulfur dioxide and ozone had similar absorption spectra, it was necessary to solve for both species simultaneously. Jim Kerr of the Atmospheric Environment Service had faced a similar problem with Brewer Spectrophotometer data. He suggested using the Brewer algorithm for the TOMS  $\text{SO}_2$  retrievals, adding two other free parameters to account for the scattering properties of the atmosphere and surface. This algorithm was later reformulated as a matrix problem (Krueger et al., 1995). With ground-based instruments using direct sunlight to measure an overhead absorber the path is simply geometric. The satellite solutions using geometric paths are approximately correct for stratospheric sulfur dioxide clouds but fail with lower altitude clouds.

Satellite-borne observations must consider other factors to determine the path. At UV wavelengths, the paths of photons are rarely geometric; from the sun to the surface and reflected to the satellite, except for snow or ice covered terrain. For more typical low reflectivity surfaces, Rayleigh scattering in the mid-troposphere returns most of the light that is not absorbed by ozone or sulfur dioxide back to space. Absorbers below the scattering layer are only partially sensed. Thus, the optical path must be computed using a multiple scattering

radiative transfer model in which the ozone and sulfur dioxide profiles are specified. The ozone profiles are known from climatology, but the sulfur dioxide profiles depend on the eruption style. Explosive eruptions generally reach the tropopause or lower stratosphere. The path is weakly dependent on altitude above the troposphere so that precise knowledge is unnecessary even for very explosive eruptions that reach the middle stratosphere. Effusive eruptions produce a cloud in the lower troposphere where knowledge of the altitude is more important. However, the path also depends on the total absorber amounts so it cannot be specified before making the retrieval.

An iterative retrieval in which a radiative transfer path is successively approximated was developed as an off-line retrieval method (Krueger et al., 2000). This makes use of special radiative transfer tables created for volcanic clouds at 5 and 20 km to represent typical effusive and explosive eruption clouds. This retrieval method is implemented in the TOMSPLOT analysis package, available from UMBC as an IDL routine. It was also used to produce the images and total SO<sub>2</sub> mass estimates used in this paper. The iterative retrievals are time consuming, so only regions containing fresh eruption clouds are normally processed this way. Whereas Fig. 1a,b,c use TOMS standard production data, the following regional figures use the off-line Iterative Retrieval data (labeled Iterative

SO<sub>2</sub>). Global figures use the standard product SOI (labeled Sulfur Dioxide Index). The figures show the exact ground resolution of the TOMS data by displaying the footprint of each observation.

#### 4. Reanalysis of the El Chichon eruption cloud TOMS data

The initial El Chichon eruption at 2332 LT on March 28 was observed in GOES infrared image data and tracked every 30 min during the course of the eruptions over the next week (Matson, 1984). The IR brightness temperatures were consistent with a plume height above the 16.5 km tropopause. The first post-eruption TOMS pass over Mexico at 1816 UT (1216 AM LT) on March 29 showed a significant sulfur dioxide cloud centered NW of the volcano and spreading both east and west (Fig. 2a). This cloud coincides in part with bright cloud patches in the GOES visible image at 1500 LT (Matson, 1984). The SO<sub>2</sub> cloud has a peak value of 192 DU; the total SO<sub>2</sub> mass in the cloud is about 720 ktons (0.72 Tg). This makes this initial eruption mass greater than the Mt. St. Helens eruption of 1980.

The TOMS AI image shows a large ash cloud that had spread northeast from the volcano over the Yucatan peninsula (Fig. 2b). This cloud coincides with the ash cloud in the GOES visible image. As

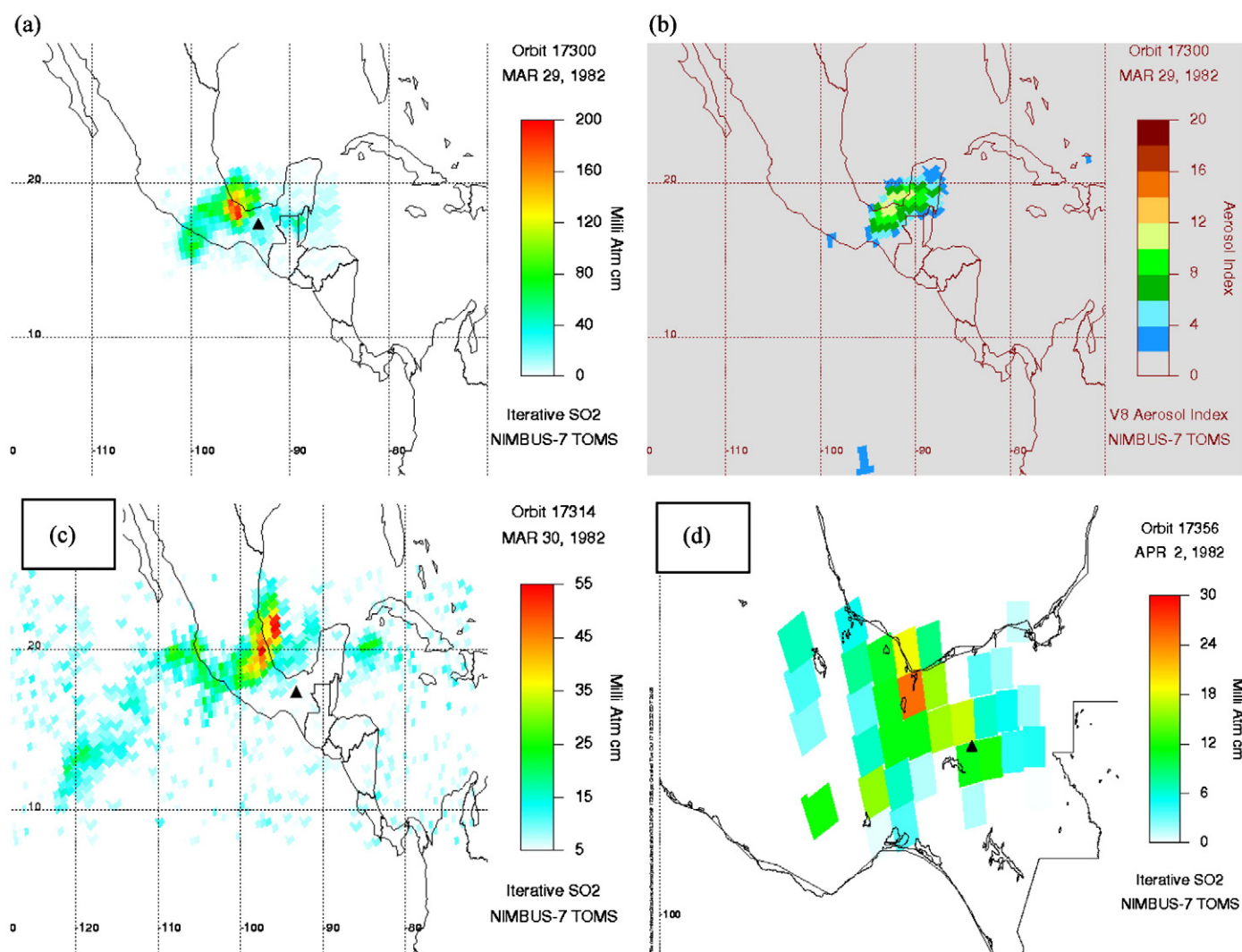


Fig. 2. a. A new SO<sub>2</sub> off-line algorithm solves simultaneously for sulfur dioxide and ozone by iteratively correcting the optical path. This image shows the iterative SO<sub>2</sub> retrieval on March 29, 1982, about 12 hours after the initial El Chichon eruption, when the cloud center NW of the volcano has a peak amount of 192 DU, almost as large as 250 DU tropical ozone amounts. b. The March 29 ash cloud drifting NE from El Chichon shown by blue, green, and yellow pixels from TOMS AI data. The blue pixels at the equator are false retrievals due to sun glint. c. On March 30 the peak SO<sub>2</sub> amounts diminish to about 50 DU as the cloud is sheared into lower altitude eastward and higher altitude westward drifting components. d. Lower level eruptive activity of El Chichon on April 2 produced this small SO<sub>2</sub> plume. The actual TOMS footprints are easily distinguished by the rectangular pixels at this map scale. (For interpretation of the references to color in this figure legend, the reader is referred to the web version of this article.)

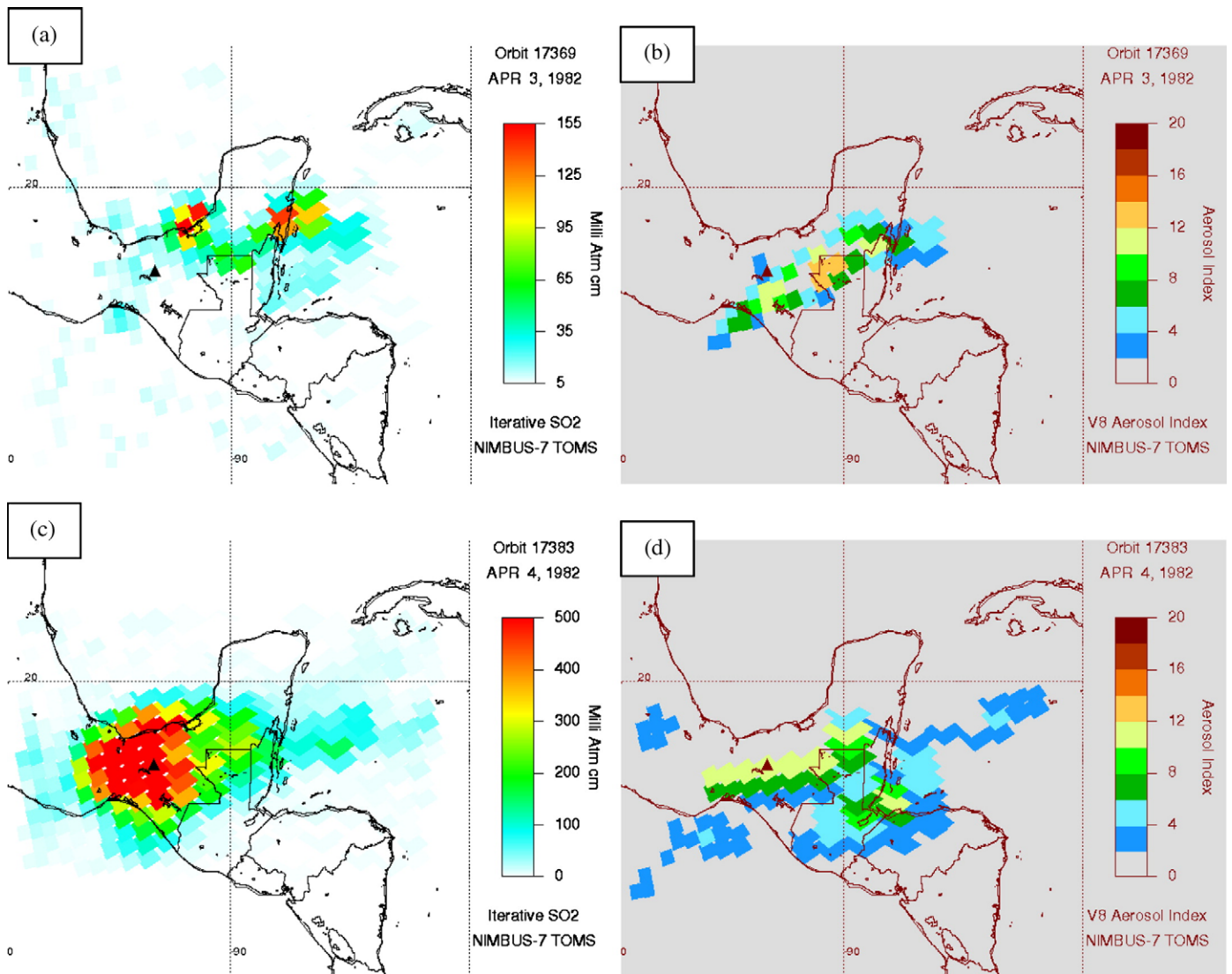


Fig. 3. a and b. A larger eruption at 0250 LT on April 3 released 0.31 Tg of SO<sub>2</sub> in these eastward-drifting upper tropospheric SO<sub>2</sub> (a) and ash (b) clouds. c and d. El Chichon's largest eruption, beginning at 0522 LT on April 4, produced dense SO<sub>2</sub> and ash clouds. Peak SO<sub>2</sub> amounts of 600 DU were found in the cloud that contained at least 3.5 Tg. The ash clouds appear south of the volcano although some of the central cloud may be missing due to failure of the TOMS ozone algorithm due to high SO<sub>2</sub> amounts.

Matson (1984) notes, the winds at Veracruz were from the southwest between 10.4 and 13.7 km and from the northeast from 20.7 to 24 km. Thus, the winds veered from westerly to easterly from the upper troposphere to the lower stratosphere. Based on the cloud drift the ash was clearly in the troposphere while the SO<sub>2</sub> was in the stratosphere.

On March 30 the previous day's SO<sub>2</sub> cloud center continued to drift slowly northwest and to spread both east and west (Fig. 2c). This is consistent with a distribution over a range of altitudes such that this plume became sheared into an east–west banner. No new SO<sub>2</sub> was found although a small explosion, possibly phreatic, was reported that morning. No ash cloud remained on March 30, suggesting a rapid fall out due to large particle sizes or aggregation of fine ash. The nearly stationary central SO<sub>2</sub> cloud was over central Mexico at a wind minimum near the tropopause; a thinner cloud at higher altitudes drifted west. The total sulfur dioxide mass on Apr 30 (Fig. 2c) was ~1.6 Tg, larger than on April 29 (Fig. 2a) as explained later in section 6.

On April 2 a small plume NW of the volcano (Fig. 2d) from renewed activity contained about 17 kt of SO<sub>2</sub> that was probably due to degassing because no new eruptive activity had been reported until later that day.

On April 3, a stronger eruption at 0250 LT produced dual clouds that drifted E and NE (Fig. 3a). These clouds, in the upper troposphere because

of the direction of motion, contained about 310 kt of SO<sub>2</sub>. The eruption also produced a large ash cloud as shown in the AI image (Fig. 3b), and observed in GOES data Matson (1984). The ash cloud appears south of the sulfur dioxide cloud due to its location in the troposphere.

El Chichon experienced its largest eruption beginning at 0522 LT on April 4. The eruption was detected 6 hours later by TOMS as a great sulfur dioxide cloud centered over the volcano trailing off primarily to the east (Fig. 3c). Peak SO<sub>2</sub> values were near 600 DU and the mass of SO<sub>2</sub> was at least 3.5 Tg. Some SO<sub>2</sub> may be masked because of the high amounts in the cloud. A large ash cloud was found in the AI image (Fig. 3d). The position corresponded with that reported by Schneider et al. (1999) from AVHRR data. The ash again was observed primarily south of the SO<sub>2</sub> plume.

The sulfur dioxide cloud center drifted slowly in a northwest direction on April 5 and expanded zonally (Fig. 4a). The cloud tonnage was 5.6 Tg showing either added SO<sub>2</sub> or unmasking as the cloud spread in area. The peak column amount on April 5 was 330 DU allowing better penetration of UV light to lower altitudes. Ash clouds (Fig. 4b) were centered SE of the volcano over Guatemala, and widely dispersed from Cuba, to the Gulf of Mexico, over northern Mexico and south over the Pacific Ocean. The Schneider et al. (1999) AVHRR analysis showed agreement with the central ash cloud, but failed to show the dispersed ash.

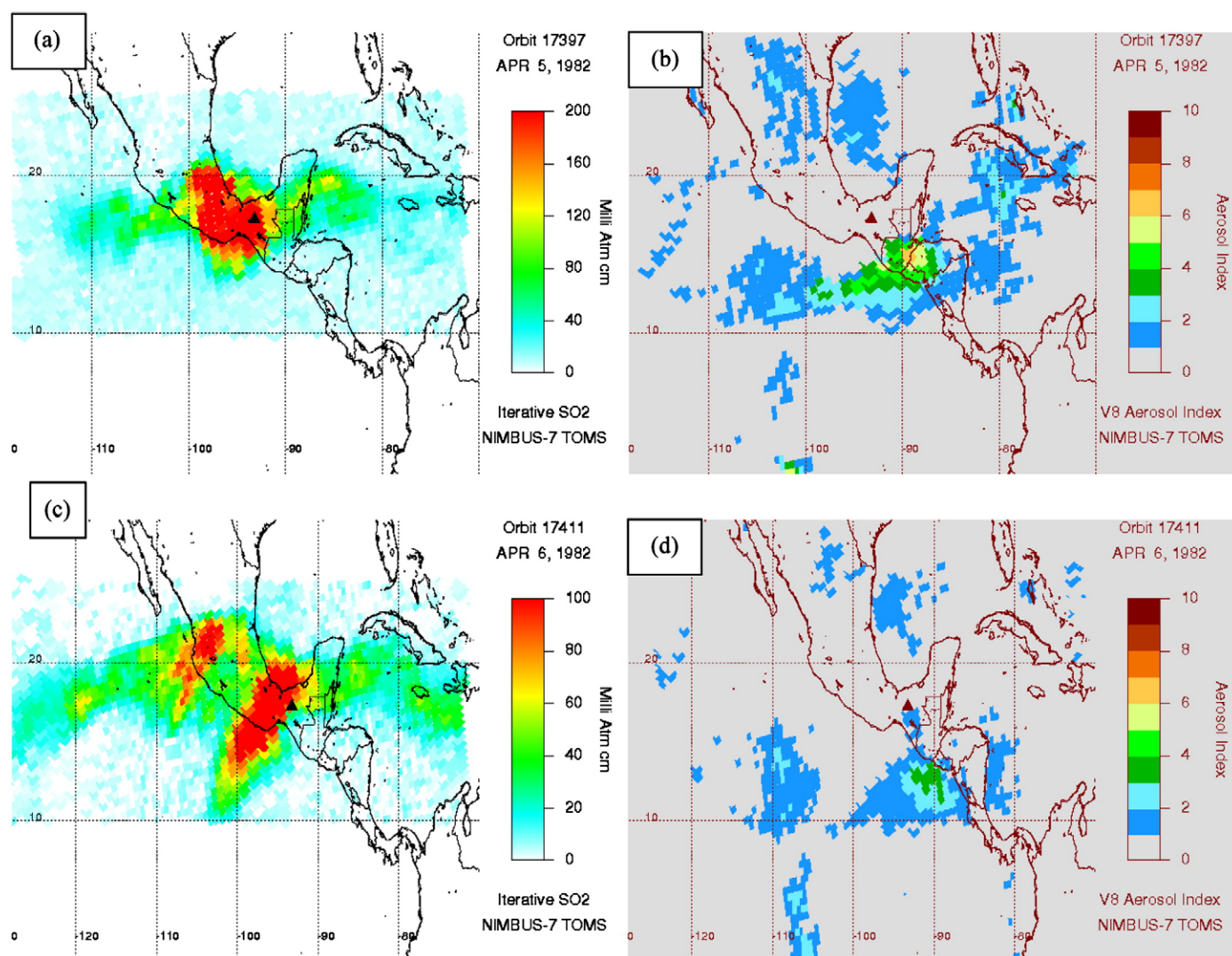


Fig. 4. a and b. On April 5 the SO<sub>2</sub> cloud has sheared to the east and west, reducing the peak amount to 330 DU. The cloud mass has increased to 5.6 Tg due either to better penetration of the cloud for remote sensing or to release of sequestered SO<sub>2</sub> on evaporation of ice crystals. The ash cloud has drifted south over Guatemala and is widely dispersed. c and d. On April 6 the SO<sub>2</sub> cloud has separated into 3 lobes, perhaps corresponding to different eruptive pulses. The ash cloud maximum remains over the Pacific Ocean.

On April 6 the stratospheric SO<sub>2</sub> cloud separated into three SW–NE trending lobes as it drifted to the west (Fig. 4c). The lobes correspond to separate volcanic events (Schneider et al., 1999) in which the highest altitude SO<sub>2</sub> is initially carried south by the dynamic perturbation of the eruption. Peak SO<sub>2</sub> amounts (184 DU) continued to drop as the cloud was sheared by the stratospheric winds. The total mass was reduced to 5.2 Tg by conversion to sulfate. The ash clouds (Fig. 4d) were now reduced in area; the densest ash cloud was off the Pacific coast of Guatemala.

On April 7 and 8 the SO<sub>2</sub> cloud lobes elongated and drifted westward. The peak values were 132 and 80 DU, respectively. The cloud mass on April 7 was 3.5 Tg. Mass estimates become more uncertain as the cloud area increases. A better perspective is gained from a simulated geostationary view from 120°W longitude on April 8 and 9 (Fig. 5a and b). Note the change in scale between the two figures. Here it is clear that the volcanic plume extended from Mexico to Hawaii.

## 5. Global motion of El Chichon clouds

The stratospheric clouds from the El Chichon eruptions were carried by easterly winds that varied with altitude from nearly zero at the tropopause to about 22 m/s at 26 km. The sulfur dioxide band was

generally contained within 10 to 30°N as it drifted across Hawaii on April 8–9, crossed the International Date Line on April 10, moved across S. Asia, India, and the Persian Gulf by April 20, then crossed Africa and the Atlantic Ocean before returning to Mexico on April 25 (Fig. 5c). This produced a global-scale banner whose head wrapped around the earth while its tail remained nearly fixed over Mexico. The initially 25 km tall eruption columns were distorted by wind shear into a thin 40,000 km long band in 3 weeks.

A similar banner was observed at visible and IR wavelengths from NOAA operational satellites (Robock and Matson, 1983) and the NASA Solar Mesosphere Explorer satellite (Barth et al., 1983). Sulfur dioxide does not absorb at these wavelengths so volcanic ash and sulfate from oxidation of sulfur dioxide must be responsible for this signal. The “dust” in the El Chichon cloud was detected in the images by slightly higher reflectivity grays over dark oceans and as a blurring of underlying clouds or surface features.

These satellite techniques tracked the same cloud as it circled the globe, arriving back over Central America on April 25. The leading edge moved 40,000 km west at 22.2 m/s, but the tail drifted only 1000 km north at 0.55 m/s. This means that the El Chichon cloud carried a mixture of fine ash, sulfate, and SO<sub>2</sub> at the same altitudes for at least one month. This extraordinary behavior has not been reported from other eruptions.

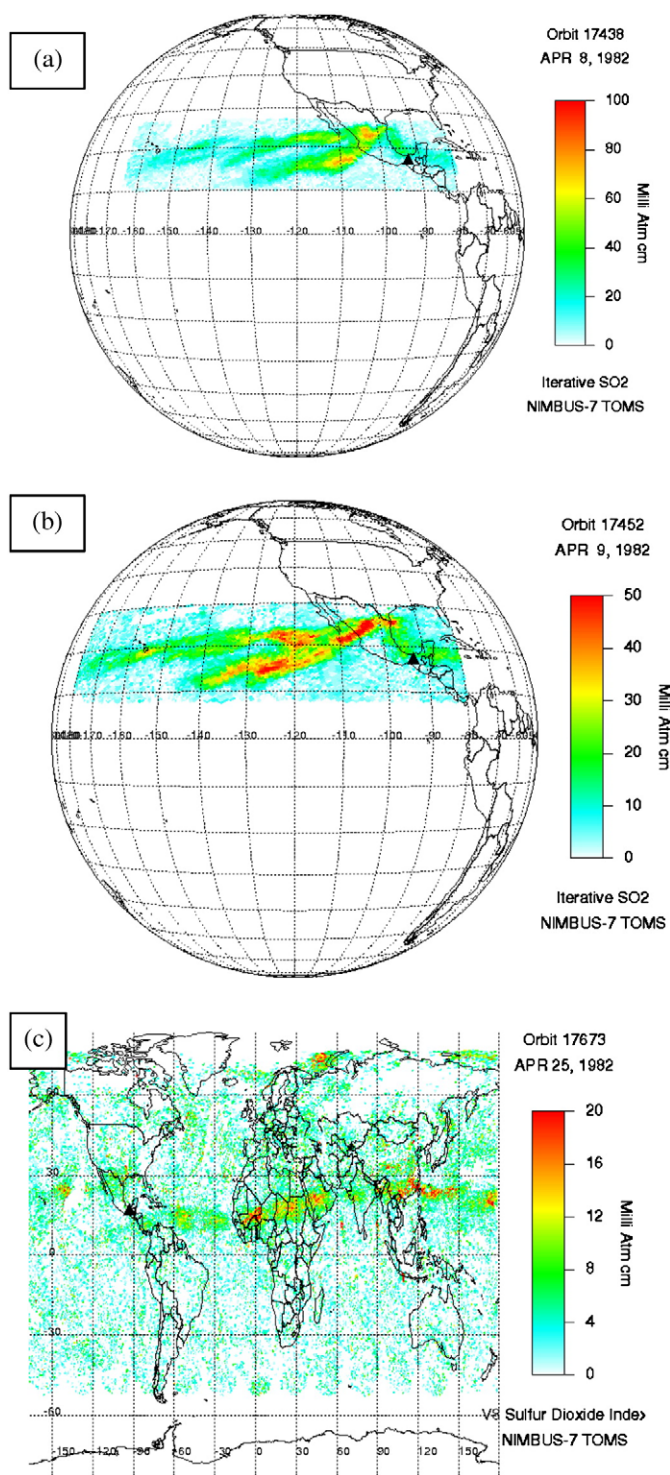


Fig. 5. a and b. Simulated geostationary view of  $\text{SO}_2$  clouds drifting west on April 8 and 9, showing arrival of the cloud at Hawaii on April 8. Note the scale is changed between images to make the cloud position clear as the peak  $\text{SO}_2$  amounts decrease with time through chemical conversion to sulfate and through dispersion. c. On April 25 the  $\text{SO}_2$  cloud front completed its first global circuit while the tail of the cloud remains rooted over Mexico. After 3 weeks the  $\text{SO}_2$  has largely been converted to sulfate aerosol that is not directly detected by TOMS, but produces a scan angle modulation of the ozone and  $\text{SO}_2$  retrievals that is visible here by the regular pattern of red features along the faintly enhanced green plume. (For interpretation of the references to color in this figure legend, the reader is referred to the web version of this article.)

The ash and sulfate aerosols were detected by lidars in Hawaii and Japan. Observers at Mauna Loa saw unusual sunrise and sunsets as early as April 5 and 6. Mauna Loa lidar data showed the appearance of

layers of aerosols on April 9 at 22 and 26 km (Coulson, 1983; Deluisi et al., 1983). The 26 km layer was first detected at Fukuoka, Japan on April 18 (Shibata et al., 1984).

## 6. Eruption mass

The initial eruption on March 28 was observed to contain 0.7 Tg  $\text{SO}_2$  about 12 hours after its start. Twenty-four hours later the expanding cloud mass was measured at 1.6 Tg. The March 29 cloud may have been too thick for a valid measurement of the total column or some  $\text{SO}_2$  may have been sequestered on ice (Guo, et al., 2004) so that the second day's total is a better measure of the eruption total. Similarly, the major April 4 eruption total is best determined on the second day when a mass of 5.6 Tg was found. The April 3 eruption cloud is relatively dispersed so a mass of 0.3 Tg is realistic. Thus, the cumulative total for all the eruptions on March 28, April 3, and April 4 is 7.5 Tg with an uncertainty of 30% (Krueger et al., 1995). This mass is substantially higher than the initial estimate (Krueger, 1983) but in good agreement with later estimates using Version 6 of the TOMS calibration (Bluth et al., 1997; Schneider et al., 1999; Carn et al., 2003). The current estimate is consistent with estimates of the mass of sulfate aerosol produced by oxidation of the sulfur dioxide (Hoffman and Rosen, 1983; Thomas et al., 1983).

## 7. Conclusions

The 1982 El Chichon eruption was exceeded in mass of sulfur dioxide only by the 1991 Pinatubo eruption during the past quarter century. El Chichon's cloud was unique, anchored near the Mexican source, but stretching westward around the earth in a tropical band that was recognizable in satellite data separately by its sulfur dioxide content and its aerosol content. The leading edge returned just south of the volcano after three weeks; the tropical sulfur dioxide band is recognizable for at least six weeks. This behavior attests to the simplicity of the tropical stratosphere circulation at this time; near zero winds at the tropopause, increasing uniformly to 22 m/s at 26 km. This occurred during the Northern Hemisphere Spring season at a time of maximum planetary wave activity, thus demonstrating the great isolation of the tropical atmosphere. The consistency of the sulfur dioxide and aerosol motion over a month is remarkable and apparently unique to this eruption.

The techniques developed following the El Chichon eruption to discriminate sulfur dioxide from ozone absorption in TOMS data have been applied to all eruptions in the 27-year TOMS database (Carn et al., 2003). This quantitative record of volcanic eruption input to the atmosphere removes one of the largest uncertainties in the global sulfur budget.

## Acknowledgements

The list of research contributors, colleagues, and collaborators is very long. Lou Walter and Charles Schnetzler of the NASA Goddard Space Flight Center (GSFC) early recognized the geophysical value of the TOMS  $\text{SO}_2$  data and encouraged the funding of this work by NASA. Jim Kerr of Atmospheric Environment Service, Toronto, suggested an algorithm for separating  $\text{SO}_2$  from ozone used with Brewer spectrophotometer data. This was modified for the satellite environment by the author and Nickolay Krotkov, including suggestions by Pawan Bhartia. Data processing algorithms and software were developed by Scott Doiron, Ian Sprod, Reggie Gallimore, and Colin Seftor. Greg Bluth was the first Post-Doc to analyze data from other eruptions. Near real-time processing methods were developed by Lonnie Bowlin and Bob Farquhar, with the strong encouragement by Mike Comberiate of GSFC and the collaboration of Tom Casadevall of US Geological Survey. Tom Simkin and Jim Luhr of the Smithsonian Institution provided conjunctive data for later eruptions. Funding was provided by NASA's Earth Sciences Directorate, including Mike Kurylo, Jack Kaye, and Shelby Tilford, who provided the funding for

the follow-on series of TOMS instruments (Meteor-3, ADEOS I, and Earth Probe) that continued the data record until 2006. Thanks to Grant Heiken and Bill Rose for excellent suggestions to improve the manuscript.

## References

- Barth, C.A., Sanders, R.W., Thomas, R.J., Thomas, G.E., Jakosky, B.M., West, R.A., 1983. Formation of the El Chichon aerosol cloud. *Geophys. Res. Lett.* 10 (11), 993–996.
- Bhartia, P.K. and Wellemeyer, C.W., 2004. Version 8 TOMS Algorithm Theoretical Basis Document, available at [http://toms.gsfc.nasa.gov/version8/version8\\_update.html](http://toms.gsfc.nasa.gov/version8/version8_update.html).
- Bluth, G.J.S., Rose, W.I., Sprod, I.E., Krueger, A.J., 1997. Stratospheric loading of sulfur from explosive volcanic eruptions. *J. Geol.* 105, 671–683.
- Carn, S.A., Krueger, A.J., Bluth, G.J.S., Schaefer, S.J., Krotkov, N.A., Watson, I.M., Datta, S., 2003. Volcanic eruption detection by the Total Ozone Mapping Spectrometer (TOMS) instruments: a 22-year record of sulphur dioxide and ash emissions. In: Oppenheimer, C., Pyle, D.M., Barclay, J. (Eds.), *Volcanic Degassing*. Geol Soc London Spec Pub, vol. 213, pp. 177–203.
- Coulson, K.L., 1983. Effects of the El Chichon volcanic cloud in the stratosphere on the polarization of light from the sky. *App. Optics* 22, 1036–1050.
- Dave, J.V., Mateer, C.L., 1967. A preliminary study on the possibility of estimating total atmospheric ozone from satellite measurements. *J. Atmos. Sci.* 24, 414–427.
- DeLuisi, J.J., Dutton, E.G., Coulson, K.L., DeFoor, T.L., Mendonca, B.G., 1983. On some radiative features of the El Chichon volcanic stratospheric dust cloud and a cloud of unknown origin observed at Mauna Loa. *J. Geophys. Res.* 88, 6769–6772.
- Guo, S., Bluth, G.J.S., Rose, W.I., Watson, I.M., Prata, A.J., 2004. Re-evaluation of SO<sub>2</sub> release of the 15 June 1991 Pinatubo eruption using ultraviolet and infrared satellite sensors. *Geochem. Geophys. Geosyst.* 5, Q04001. doi:10.1029/2003GC000654.
- Heath, D.F., Krueger, A.J., Roeder, H.R., Henderson, B.D., 1975. The Solar Backscatter Ultraviolet and Total Ozone Mapping Spectrometer (SBUV/TOMS) for Nimbus G. *Opt. Eng.* 14, 323–331.
- Hofmann, D.J., 1987. Perturbations to the global atmosphere associated with the El Chichon volcanic eruption of 1982. *Rev. Geophys.* 25 (4), 743–759.
- Hoffmann, D.J., Rosen, J.M., 1983. Stratospheric sulfuric acid fraction and mass estimate for the 1982 volcanic eruption of El Chichon. *Geophys. Res. Lett.* 10, 313–316.
- Krueger, A.J., 1983. Sighting of El Chichon sulfur dioxide with the Nimbus-7 total ozone mapping spectrometer. *Science* 220, 1377–1378.
- Krueger, A.J., 1989. The global distribution of total ozone: TOMS satellite measurements. *Planet. Space Sci.* 37, 1555–1565.
- Krueger, A.J., Walter, L.S., Bhartia, P.K., Schnetzler, C.C., Krotkov, N.A., Sprod, I., Bluth, G.J.S., 1995. Volcanic sulfur dioxide measurements from the Total Ozone Mapping Spectrometer (TOMS) Instruments. *J. Geophys. Res.* 100, 14,057–14,076.
- Krueger, A.J., Schaefer, S.J., Krotkov, N.A., Bluth, G., Barker, S., 2000. Ultraviolet Remote Sensing of Volcanic Emissions. In: Mouginiis-Mark, P.J., Crisp, J.A., Fink, J. H. (Eds.), *Remote Sensing of Active Volcanism*, AGU Geophysical Monograph, vol. 116, pp. 25–43.
- Luhr, J.F., Carmichael, I.S.E., Varekamp, J.C., 1984. The 1982 eruptions of El Chichón Volcano, Chiapas, Mexico: mineralogy and petrology of the anhydrite-bearing pumices. *J. Volcanol. Geotherm. Res.* 23, 68–108.
- Matson, M., 1984. The 1982 El Chichon volcano eruptions – a satellite perspective. *J. Volcanol. Geotherm. Res.* 23, 1–10.
- McGee, T., Burris, J., 1987. SO<sub>2</sub> absorption cross sections in the near UV. *J. Quant Spectrosc. Radiat. Transfer* 37, 165–182.
- McPeters, R.D., Bhartia, P.K., Krueger, A.J., Herman, J.R., Schlesinger, B.M., Wellemeyer, C. G., Seftor, C.J., Jaross, G., Taylor, S.L., Swisler, T., Torres, O., Labow, G., Byerly, W., Cebula, R.P., 1993. *Nimbus-7 Total Ozone Mapping Spectrometer (TOMS) Data Products User's Guide*, NASA Ref. Pub. 1323.
- Robock, A., Matson, M., 1983. Circumglobal transport of the El Chichon volcanic dust cloud. *Science* 221, 195–197.
- Rose, W.I., Bornhorst, T.J., Halsor, S.P., Capaul, W.A., Plumley, P.S., Dela Cruz-Reyna, S., Mena, M., Mota, R., 1984. Volcán El Chichón, Mexico: pre-1982 S-rich eruptive activity. *J. Volcan. Geotherm. Res.* 23, 147–149.
- Schneider, D.J., Rose, W.I., Coke, L.R., Bluth, G.J.S., Sprod, I.E., Krueger, A.J., 1999. Early evolution of a stratospheric volcanic eruption cloud as observed with TOMS and AVHRR. *J. Geophys. Res.* 104, 4037–4050.
- Shibata, F., Fujiwara, M., Hirono, M., 1984. The El Chichon volcanic cloud in the stratosphere: lidar observation at Fukuoka and numerical simulation. *J. Atmos. Terr. Phys.* 46, 1121–1146.
- Sigurdsson, H., Carey, S.N., Espindola, J.M., 1984. The 1982 eruptions of El Chichón Volcano, Mexico: stratigraphy of pyroclastic deposits. *J. Volcano. Geotherm. Res.* 23, 11–37.
- Thomas, G.E., Jakosky, B.M., West, R.A., Sanders, R.W., 1983. Satellite limb-scanning thermal infrared observations of the El Chichon stratospheric aerosol: first results. *Geophys. Res. Lett.* 10 (11), 997–1000.
- Varekamp, J.C., Luhr, J.F., Prestegard, K.L., 1984. The 1982 eruptions of El Chichon Volcano (Chiapas, Mexico): character of the eruptions, ash-fall deposits, and gasphase. *J. Volcanol. Geotherm. Res.* 23, 39–68.
- Wu, C.Y.R., Judge, D.L., 1981. SO<sub>2</sub> and CS<sub>2</sub> cross section data in the ultraviolet region. *Geophys. Res. Lett.* 8 (7), 769–771.